

Morphological aspects of the coronary artery in neonates

A. Avirmed, D. Amgalanbaatar, S. Enebish, B. Och, N. Narantuya,
E. Plunkett, K. Plunkett

Health Sciences University of Mongolia

[Received 15 November 2006; Revised 23 September 2007; Accepted 24 October 2007]

Knowledge of the morphometric quantities of the coronary arteries in neonates is an increasingly vital component in the management of congenital and acquired heart disease. Because of the considerable heterogeneity of coronary vasculature, what is considered atypical and aberrant or insignificant anatomy is often unclear. The purpose of our present study is to define the normal anatomy of neonates. This was done by focusing on segment analysis of the coronary arteries, which was used to obtain accurate definitions of the length and diameter of the coronary network. The lengths, widths and numbers of collateral branches of the coronary arteries of neonates were measured. The coronary vessels of 50 neonate hearts were visualised post mortem by injection of the coronary arteries with opaque X-ray dye for the imaging study. Black ink cast and silver impregnation specimens were also studied. The longest segment of the circumflex branches of the left coronary arteries was the first, the lengths measuring $7188.5 \pm 839.6 \mu\text{m}$ and the diameters $850 \pm 90.8 \mu\text{m}$. The lengths of segments II, III and IV were $5780 \pm 1182.7 \mu\text{m}$, $5397.5 \pm 2070.2 \mu\text{m}$ and $6932.8 \pm 2236.5 \mu\text{m}$ and the diameters were $680 \pm 90.8 \mu\text{m}$, $510 \pm 90.8 \mu\text{m}$ and $408 \pm 77.58 \mu\text{m}$ respectively. The longest segment of the anterior interventricular branches of the left coronary arteries was the first, with lengths of $10151.4 \pm 1298.6 \mu\text{m}$ and diameters of $1141.9 \pm 82.1 \mu\text{m}$. The lengths of segments II, III and IV were $8208.5 \pm 1222.3 \mu\text{m}$, $3278.5 \pm 602.4 \mu\text{m}$ and $5370 \pm 1657.6 \mu\text{m}$ and the diameters were $971 \pm 82.1 \mu\text{m}$, $801.42 \pm 82.1 \mu\text{m}$ and $631.4 \pm 82.1 \mu\text{m}$ respectively. The lateral branches were increased in number in the fourth segment. Its diameters ranged from $157.8 \pm 31.7 \mu\text{m}$ to $655.7 \pm 99.7 \mu\text{m}$. The main branch of the right coronary artery was short at the base of the heart. In the newborn the lateral branches of the right coronary artery were short, scattered and curved. Analysis of the data suggests a new anatomical system for classifying the vasculature of the coronary arteries in neonates.

Key words: heart, coronary arteries, black ink, X-ray examination, morphometric study

INTRODUCTION

The coronary arteries of the human heart and their branching characteristics have been the subject of particular attention among researchers [2–4, 7, 18, 20, 21, 33, 36–38, 40, 41, 43, 44]. The finer details may be of interest to anatomists and radio-

logists, but in clinical practice surgeons need only be concerned with some of the more constant and important features. The branching characteristics of the coronary arterial tree play an important role in cardiac operations, such as heart pacemaker implantation, angioplasty and even stent placement [15].

Table 1. The lengths and diameters of heart muscle microcirculation in neonates

Values		Cardiac muscle of the left ventricle			Cardiac muscle of the right ventricle			Inter ventricular septum	
		External	Circular	Internal	External	Circular	Internal	Right part	Left part
Diameters of arterioles	Diameter [μm]	23 \pm 0.4	24 \pm 0.4	22 \pm 0.3	23 \pm 0.4	24 \pm 0.5	23 \pm 0.4	23 \pm 0.4	25 \pm 0.6
Diameters of meta-arterioles	Diameter [μm]	12 \pm 0.3	12 \pm 0.3	13 \pm 0.3	12 \pm 0.2	13 \pm 0.3	12 \pm 0.2	12 \pm 0.4	12 \pm 0.3
Diameters of capillaries	Diameter [μm]	4.96 \pm 0.1	4.87 \pm 0.1	4.95 \pm 0.1	5.1 \pm 0.3	5.1 \pm 0.1	5.1 \pm 0.1	5.0 \pm 0.1	5.1 \pm 0.1
The lengths and widths of capillary loops	Width	15.5 \pm 0.3	14.4 \pm 0.6	16 \pm 0.4	15.3 \pm 0.4	15 \pm 0.5	16 \pm 0.5	16 \pm 0.6	14 \pm 0.4
	Length	74 \pm 1	74 \pm 1	88 \pm 2	72 \pm 2	85 \pm 2	75 \pm 1	77 \pm 2	71 \pm 1.1

It is difficult to evaluate the microcirculation of the heart in the newborn. The available knowledge base is inadequate at present. The black ink cast technique has been applied most frequently to studies of microcirculation. In the present study we have focused on learning about the architecture of the small coronary arteries in the newborn. The eventual focus will be on modification of the silver impregnation method proposed by Kuprianov, in which the anatomical sections are pre-treated with silver nitrate. This procedure enhances the penetration and improves the detection of the structures of the walls of the micro vessels of the blood.

Ethical issues

In accordance with the guidelines for research involving human subjects or human biological materials the Ethics Committee of the Health Sciences University of Mongolia, approved the aims and procedures of the study.

MATERIAL AND METHODS

The research study was implemented at the Department of Morphology, the Health Sciences University of Mongolia, the Maternal and Child Health Research Centre, Mongolia and the National Forensic Medicine Bureau of Mongolia. The study obtained 50 human hearts of both sexes (19 male and 31 female) from cadavers of neonates who had died of non-cardiovascular disease (Table 1). The study enrolled the newborn, defined as individuals aged from 0 to 10 days (5.4 ± 1.4), a period which has been revised and expanded by researchers [13].

Thanks to co-operation on the part of the organisations mentioned above the following criteria for obtaining hearts were fulfilled:

- the organs were obtained within four hours of death, the above-mentioned ethical criteria were fulfilled and the hearts were examined;
- an organ was excluded from the study if the coronary arteries showed any macroscopic signs of congenital anomaly. The morphometric study was performed by the method recommended by scholars [1, 9, 12].

To achieve the goal of defining the microcirculation, we used the black ink cast method in some hearts to assess the microcirculation, a modified silver impregnation method in some of the hearts to define the wall structure of the micro-blood vessels and the coronary angiography method in the remainder of the hearts to determine the anatomy of the coronary arteries and their main branches.

Although the black ink cast method was used to define the microcirculation, it did not reveal information about the wall structure of the heart's micro-blood vessels. The silver impregnation technique is most frequently applied to solve this, as it evaluates the wall structure of the micro-blood vessels more effectively.

We used the coronary angiography method in some hearts to determine the morphology of the great arteries such as the right and left coronary arteries and their derived branches.

The coronary angiography method

The heart was isolated and immediately processed. The ascending aorta having been opened, 2 or 3 glass cannulae were introduced into the right

and left coronary arteries. The cannulae were ligated tightly in the bulbous aorta where the coronary artery originated and connected to a plastic connector. One end of each tube was connected to a 10 ml syringe. The cardiac vascular system was perfused with 10 ml of 5% contrast media of (10.0 g glycerin, 1.0–2.0 g PbO_2) at 80–100 mm Hg pressure. In selected cases barium sulphate was used as the opaque media. X-ray films were then made using the URD-110 X-ray unit. These methods of opening and taking X-ray films have been described by earlier researchers [45]. All the procedures were performed under the control of an X-ray technician.

Black ink cast

By this method [31] the first cut was performed at the level of the pericardial sac. The pulmonary artery was then removed and the ascending aorta was cut through the anterior and posterior walls. Next cannulae were introduced into the left and right coronary arteries. The great vessels were tied to prevent black ink flowing out of the vasa vasorum (the walls of the great vessels). The cannulae were additionally inserted into the right and left coronary arteries and ligated tightly. Injection with a water suspension of black ink (1:3) was performed under manometric control. To improve the results, the ink was filtered three times prior to injection. After the infusion procedure with black ink, the cannulae were removed and the vessels ligated.

After fixation in 10% formaldehyde for 14 days, the heart tissue was cut with a specially adapted circular saw into 1 cm^3 blocks and then into 30–60 μm thin blocks. In this way the microcirculation of the heart was studied.

Kuprianov's silver impregnation method

According to the silver impregnation method [27], the heart tissue was cut with a specially adapted circular saw into 1 cm^3 blocks and then into 5–10 μm thin blocks. The following steps were used for the silver impregnation method of Kuprianov:

- the heart tissue blocks were fixed in 2% formaldehyde (PH = 7.2) for one day;
- they were rinsed 2–3 times in tap water;
- they were gently submerged in distilled water 2–3 times;
- the specimens were then stained in a 10–15% silver nitrate solution and transferred into a container at 37°C;
- the specimens were rinsed with distilled water for 3 min;

- the specimens were kept in 1% formaldehyde (PH < 7) until no remnants of soft tissue were visible;
- they were kept in silver nitrate for 2 min;
- they were pretreated in 0.5% formaldehyde (PH < 7) and kept at 23°;
- finally the specimens were placed in 0.5% formaldehyde (PH < 7) until the colours turned to yellow. If the specimens were thin, they were kept until they turned brown.

Data management

Data analysis was performed with a computer program, SPSS version 11. A p value of 0.05 and 0.01 was used to indicate statistical significance for all the parameters evaluated.

RESULTS

The diameters of the *arteria coronaria dextra* (right coronary arteries), *ramus circumflexus* (circumflex branches of the coronary artery) and *ramus interventricularis anterior* (anterior interventricular branches of the left coronary artery) were assessed using segment analysis according to the WHO recommendation. We divided the whole vessel into 4 segments and measured the diameter, length and number of the collateral branches of each segment. A vessel segment was defined in order of the vessel diameters. The probability of the changing parts of the vessel diameters were calculated by means of the following formula:

$$t = \frac{M_1 - M_2}{\sqrt{m_1^2 + m_2^2}}$$

t — Student's t test; M_1 — arithmetic mean at the beginning of the segment; M_2 — arithmetic mean at the end of the segment; m_1 — standard error of the arithmetic mean at the beginning of the segment; m_2 — standard error of the arithmetic mean at the end of the segment

Arteria coronaria dextra (the right coronary artery)

The right coronary artery (RCA) originates from the bulbous aorta and runs in the coronary groove to go around the right border of the heart and reach the crux of the heart. It supplies blood to the inferior (diaphragmatic) right ventricular wall and often the posterior third of the interventricular septum as well as the free wall of the right ventricle through its right ventricular (acute marginal) branches (Fig. 1).

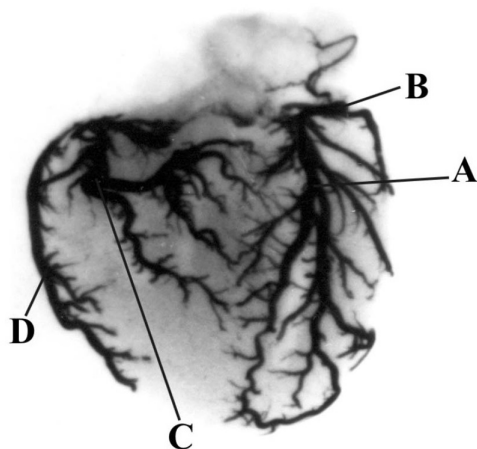


Figure 1. X-ray film of the coronary artery in neonates. Anterior position; A — anterior interventricular branch of the left coronary artery; B — circumflex branch of the left coronary artery; C — posterior interventricular branch of the left coronary artery; D — marginal branch.

The main branch of RCA was short at the base of the heart. In neonates the lateral branches of RCA were short, scattered and curved. This produced poor blood supply to the apex of the heart. The longest segment was segment IV, with lengths of $7625 \pm 1560 \mu\text{m}$ and diameters of 793.3 ± 158.6 . The lengths of the first, second and third segments were $5751.6 \pm 634.5 \mu\text{m}$, $5893.3 \pm 1192.4 \mu\text{m}$ and $5808.3 \pm 1416.3 \mu\text{m}$, the diameters were $1303.3 \pm 158.6 \mu\text{m}$, $1133.3 \pm 158.6 \mu\text{m}$, and $963.3 \pm 158.6 \mu\text{m}$ respectively. The lateral branches increased in number in the IV segment. The diameter of the lateral branches of RCA ranged from $238 \pm 37.2 \mu\text{m}$ to $510 \pm 113.3 \mu\text{m}$.

The left main coronary artery

The left main coronary artery branched off the bulbous aorta, coursed 5 mm in length and divided further into two major branches, the anterior interventricular branch and a circumflex branch. The left main coronary artery did not resemble the left coronary artery in adults, and for this reason we measured the left coronary artery via these two arteries.

Ramus circumflexus (the circumflex branch of the left coronary artery)

The circumflex branch of the left coronary artery courses along the coronary groove, around the left border of the heart, and posteriorly toward the crux of the heart. The circumflex branch of the left coronary artery should reach the crux of the heart and supply the posterior wall of the left ventricle (Fig. 1).

Sometimes it joins the posterior interventricular branch of the coronary artery in the dorsal wall of the left ventricle. The rates of branching and ramification were low and there were few lateral branches. The longest segment of the circumflex branches of the left coronary arteries was the first, the lengths being $7188.5 \pm 839.6 \mu\text{m}$ and the diameters $850 \pm 90.8 \mu\text{m}$. The lengths of segments II, III and IV were $5780 \pm 1182.7 \mu\text{m}$, $5397.5 \pm 2070.2 \mu\text{m}$ and $6932.8 \pm 2236.5 \mu\text{m}$ and the diameters were $680 \pm 90.8 \mu\text{m}$, $510 \pm 90.8 \mu\text{m}$ and $408 \pm 77.58 \mu\text{m}$ respectively. The lateral branches increased in number in the first and second segments and diameters ranged from $198.3 \pm 43.2 \mu\text{m}$ to $412.8 \pm 58.05 \mu\text{m}$.

Ramus interventricularis anterior (the anterior interventricular branch of the left coronary artery)

The anterior interventricular branch is longer than the other branches and supplies blood to the anterior wall of the left ventricle and the anterior two thirds of the interventricular septum and, on reaching the apex of the heart, then supplies the posterior third of the interventricular septum (Fig. 1). The longest segment is the first, with lengths of $10151.4 \pm 1298.6 \mu\text{m}$ and diameters of $1141.9 \pm 82.1 \mu\text{m}$. The lengths of segments II, III and IV were $8208.5 \pm 1222.3 \mu\text{m}$, $3278.5 \pm 602.4 \mu\text{m}$ and $5370 \pm 1657.6 \mu\text{m}$ and the diameters were $971 \pm 82.1 \mu\text{m}$, $801.42 \pm 82.1 \mu\text{m}$ and $631.4 \pm 82.1 \mu\text{m}$ respectively. The lateral branches increased in number in the fourth segment and its diameters ranged from $157.8 \pm 31.7 \mu\text{m}$ to $655.7 \pm 99.7 \mu\text{m}$.

Arteriole and meta-arteriole

The arterioles were distributed at an acute angle to the muscle fibres and were therefore not distinguishable from each other in their diameter. The arterioles with tiny diameters gave off a dichotomous and tree-like branching pattern before ramification into meta-arterioles (Fig. 2). This branching pattern was seen in the circular and internal longitudinal layer of the left myocardium. In the silver impregnated specimens a layer of smooth muscle cells with their nuclei was seen in the walls of the arterioles (Fig. 3). This depended on the diameter of the arterioles and as this narrowed the distribution of the nuclei changed in shape from irregular to spiral.

The diameters of the arteriole and meta-arterioles in the layers of the heart myocardium in neonates are shown in Table 1.

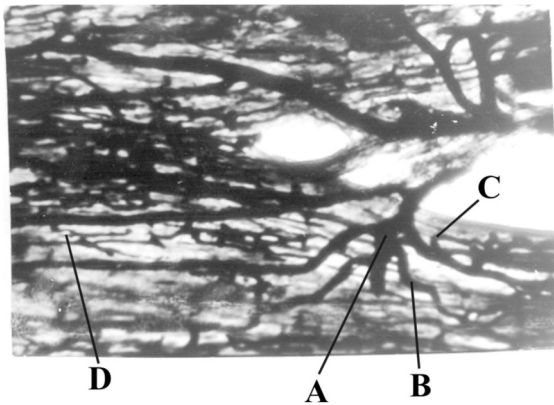


Figure 2. Photomicrograph of a tree-like branching pattern of arterioles in external, longitudinal layer of the left ventricle in neonates; black-ink cast (1:3), magnification is x 40; A — arteriole I; B — arteriole II; C — meta-arteriole; D — capillary loop.

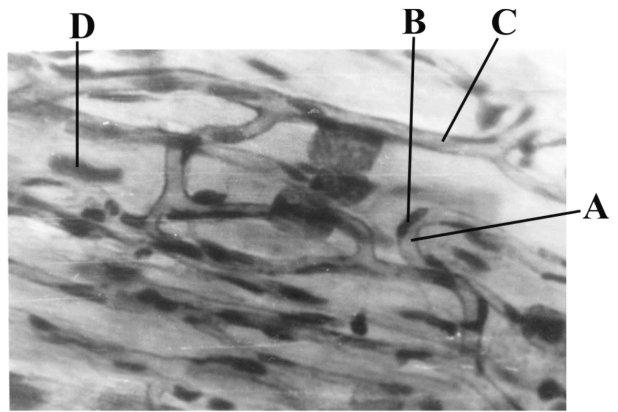


Figure 4. Photomicrograph of capillary network in external and longitudinal layer of right ventricle in neonates; silver impregnation of the vessels was performed by the Kuprianov's method, magnification is x 150; A — capillary loop; B — endothelial cell nuclei; C — large capillary; D — cardiac muscle fibre nuclei.

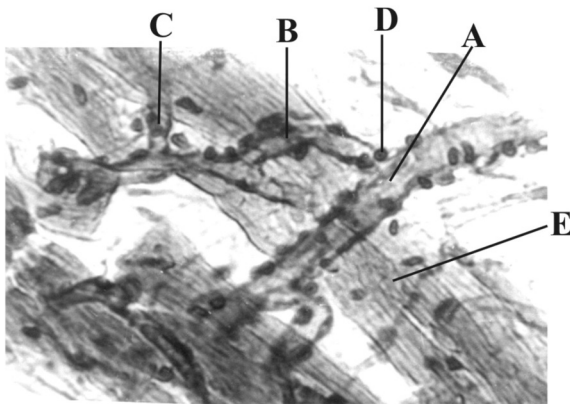


Figure 3. Photomicrograph of meta-arterioles begins from the arterioles in longitudinal layer of the left ventricle in neonates; silver impregnation of the vessels was performed according to a method recommended by Kuprianov, x 150; A — arteriole; B — meta-arteriole; C — capillary; D — meta-arteriole sphincter; E — muscle fibres.

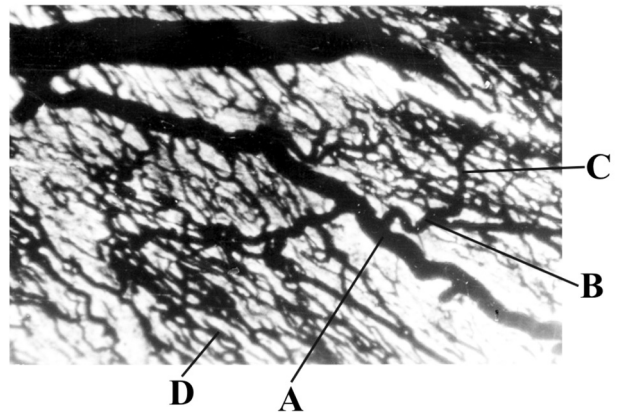


Figure 5. Photomicrograph of a dichotomous branching pattern of arterioles in external longitudinal layer of the left ventricle in neonates; black-ink cast (1:3), magnification is x 40; A — arteriole I; B — arteriole II; C — meta-arteriole; D — capillary loop.

Capillaries

The capillaries of the right ventricle were similar to those of the left ventricle and formed a network (Fig. 4), which was frequently oriented parallel to the muscle fibres (Fig. 4–6). The capillary diameters and sizes of the capillary loops in the layer of myocardium in neonates are shown in Table 1.

The capillaries emerge from arterioles or meta-arterioles and do not follow a direct route from the arterioles to the venous capillaries. At their sites of origin a ring of smooth muscle fibres called sphincter meta-arterioles controls the flow of blood entering a capillary. This is shown in Figure 3.

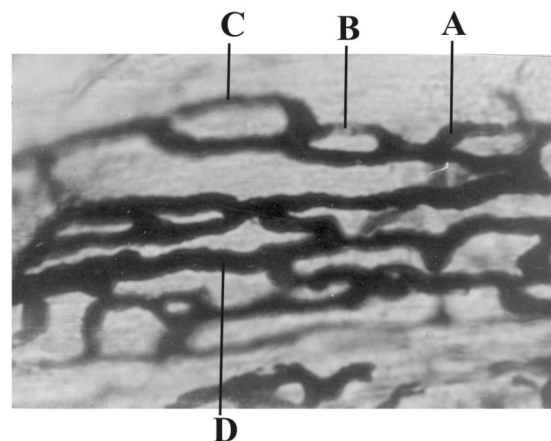


Figure 6. Photomicrograph of capillary loops in internal and longitudinal layer of left ventricle in neonates; black ink cast (1:3), magnification x 150; A — capillary; B — small capillary loop; C — large capillary loop; D — meta-arteriole.

DISCUSSION

The key observation of this study is the segment analysis of the left and right coronary arteries and their derived branches, such as the circumflex branch and anterior interventricular branches of the left coronary artery, in neonates. On the other hand, the study facilitated the classic description of the coronary arteries in the newborn in terms of diameters, lengths, number and their derived quantities. The main feature of our segment analysis is that it also provides a means of using the average morphometric parameters, those available to the management of cardiac surgery and radiology, to make cardiac simulations [30]. Furthermore, the segmentation of vessels helps to provide morphometric measurements of statistical significance. It therefore provides basic data for constructing an arterial tree model [14, 26, 29, 32].

Some studies have focused on the morphometry of the coronary as well as the pulmonary venous system [5, 6, 17, 22]. Many excellent studies have been carried out in different species [11, 16, 18, 19, 23–25, 28, 35] dealing with segment analysis of the myocardium [10, 18]. Segment analysis of the coronary artery in particular has been evaluated in only a few studies [34, 38, 39, 42], and these do not provide the necessary information for appropriate systematisation of coronary artery measurements.

The morphometric quantities of the microcirculation in neonates have been studied by a modified silver impregnation method. Understanding the heart microcirculation is important in guiding the management of the sudden death of neonates and has enhanced understanding so that operative outcomes are improved [8]. We determined the anatomical data of microcirculations in neonates by conducting studies with silver impregnation. The arterioles gave off a dichotomous branching pattern in the internal longitudinal layer of the left myocardium. This arrangement has also been reported by other researchers [40].

The arterioles were distributed at an acute angle to the muscle fibres. Those arterioles with tiny diameters gave off a tree-like branching pattern before ramification into meta-arterioles. This branching pattern was seen in the circular and internal longitudinal layers of the left myocardium. This arrangement was also noted by Zamir et al. [40].

In contrast, the present results show that the small arterioles, at least those of the terminal coronary bed which supply the heart muscle, were not identical to each other and ramified two or three times, giving a dichotomous branch. This is similar to cases reported elsewhere [3, 21, 32, 40]. In silver impregnated

specimens a layer of smooth muscle cells with their nuclei was seen in the walls of the arterioles. This was dependent on the diameter of the arterioles.

The capillaries formed a network. This network of capillaries is frequently oriented parallel to the muscle fibres. This finding is a new aspect of coronary artery distribution and is in accordance with findings reported in a recent study by Zamir [41], although his findings refer to RCA, while our study was focused on the right and left coronary arteries. Hence the parameters evaluated in this study will serve as a new basis for cardiovascular modelling [14, 18, 19, 24, 32]. We may suggest that the circumflex branch of the left coronary artery reaches the crux of the heart and supplies the posterior wall of the left ventricle. Sometimes it joins with the posterior interventricular branch of the coronary artery in the dorsal wall of the left ventricle. This is an unusual course of the circumflex branch of the left coronary artery and does not occur in adults. The main branch of RCA was short at the base of the heart. In the newborn lateral branches of RCA were short, scattered and curved. This produced poor blood supply to the apex of the heart. This study is planned and will be performed in the near future.

REFERENCES

1. Abrikosow AI (1936) Technika patologio-anatomiczeskich wskrytij trupow. Biomedic, 1: 167–174.
2. Aharinejad S, Lametschwandtner A Microvascular (1991) Casting in scanning electron microscopy. Techniques and Applications. Springer, New York, pp. 52–102.
3. Aharinejad S, MacDonald IC, MacKay CE, Mason-Savas A (1993) New aspects of microvascular casting. A scanning, transmission electron, and high-resolution intravital video microscopic study. Microsc Res Tech, 26: 473–488.
4. Aharinejad S, MacDonald IC, Schmidt EE, Bock P, Hagen D, Groom AC (1993) Scanning and transmission electron microscopy and high resolution intra-vital electron microscopy of capillaries in the mouse exocrine pancreas, with special emphasis on endothelial cells. Anat Rec, 2: 163–177.
5. Aharinejad S, Schraufnagel DE, Miksovsky A, Larson ED K, Marks SC Jr (1995) Endothelin-1 focally constricts pulmonary veins. J Thorac Cardiovasc Surg, 11: 148–156.
6. Aharinejad S, Schraufnagel DE, MacKay CA, Larson EK, Miksovsky A, Marks SC Jr (1996) Spontaneous hypertensive rats develop pulmonary hypertension associated with hypertrophied pulmonary venous sphincters, Am J Pathol, 45: 281–290.
7. Aharinejad S, Schreiner W, Neumann F (1998) Morphometry of human coronary arterial trees. Anat Res, 251: 50–59.
8. Andrew N (2006) Coronary artery anomalies. Am J Physiol Heart Circ Physiol, 287: 1014–1042.

9. Awtandilow GG (1990) Medicinskaja morfometrija, M, pp. 25–77.
10. Bassingthwaighe JB, Malone MA, Moffett TC, King RB, Little SE, Link JM, Krohn KA (1987) Validity of microsphere depositions for regional myocardial flows. *Am J Physiol*, 253: 184–193.
11. Bertuglia S, Colantuoni A, Intaglietta M (1994) Effects of L-NMMA and indomethacin on arteriolar vasomotion in skeletal muscle microcirculation of conscious and anesthetized hamsters. *Microvasc Res*, 48: 68–84.
12. Bunak WW (1931) Metodika antropologicznych issledowanij, *Bio-Medgiz*, 1: 222.
13. Bunak WW (1941) Antropometrija, *Uczpedic*, 17: 5–25.
14. Changizi MA, Cherniak C (2000) Modeling the large-scale geometry of human coronary arteries. *Can J Physiol Pharmacol*, 78: 603–611.
15. Coma-Canella I, Maceiva A, Diaz Dorronsoro Galabug J, Martinez A (1999) Changes in the diameter of the coronary arteries in heart transplant recipients with angiographically normal vessels during five years. *Esp Cardiol*, 52: 485–492.
16. Frobert O, Gregersen H, Bjerre J, Bagger TP, Kassab GS (1998) Relation between zero-stress state and branching order of porcine left coronary arterial tree. *Ann J Physiol*, 275: H2283–H2290.
17. Gustafsson H, Mulvany J, Nilsson H (1993) Rhythmic contractions of isolated small arteries: influence of the endothelium. *Acta Physiol Scand*, 148: 153–163.
18. Kaimovitz B, Lanir Y, Kassab GS (2005) Large scale 3 D geometric reconstruction of the porcine coronary arterial vasculature based on detailed anatomical data. *Ann Biomed Eng*, 33: 1517–1535.
19. Kalsho G, Kassab GS (2004) Bifurcation asymmetry of the porcine coronary vasculature and its implications on coronary flow heterogeneity. *Am J Physiol Heart Circ Physiol*, 287: H2493–H2500.
20. Kassab GS, Rider CA, Tang NJ, Fung YCB (1993) Morphometry of coronary arterial trees. *Am J Physiol*, 265: 350–365.
21. Kassab GS (2000) The coronary vasculature and its reconstruction. *Ann Biomed Eng*, 28: 903–915.
22. Kassab GS, Lin DH, Fung YC (1994) Morphometry of coronary venous system. *Am J Physiol*, 267: H2100–H2113.
23. Kassab GS, Rider CA, Jang NJ, Fung YC (1997) Morphometry of pig coronary arterial trees. *Am J Physiol*, 265: H350–H365.
24. Kassab GS, Fung YC (1994) Topology and dimensions of pig coronary capillary network. *Am J Physiol*, 267: 319–325.
25. Kassab GS, Pallencave E, Schatz A, Fung YC (1997) Longitudinal position matrix of the pig coronary vasculature and its hemodynamic implications. *Am J Physiol*, 273: H2832–H2842.
26. Karch R, Neumann F, Neumann M, Schreiner W (2000) Staged growth of optimized arteriole model trees. *Ann Biomed Eng*, 28: 495–411.
27. Kuprianow WW (1969) Puti mikrocirkuljacii. *Karta moldowenjaske. Kisziniew*, 4: 257–310.
28. Less JR, Skalak TC, Sevick EM, Jain RK (1991) Microvascular architecture in a mammary carcinoma: branching patterns and vessel dimensions. *Cancer Res*, 51: 265–273.
29. Mittal N, Zhou Y, Unga S, Linares C, Molloy S, Kassab GS (2005) A computer reconstruction of the entire coronary arterial tree based on detailed morphometric data. *Ann Biomed Eng*, 33: 1015–1026.
30. Morioka CA, Abbey Ck, Eckstein M, Close Whiting JS, Lefee M (2000) Simulating coronary arteries in X-ray angiograms. *Med Phys*, 27: 2438–2444.
31. Ogniew BW (1960) Frauczi topograficzeskaja i kliniczeskaja anatomija, M, *Medgiz*.
32. Smith NP, Pullan AJ, Hunter PJ (2000) Generation of an anatomically based geometric coronary model. *Ann Biomed Eng*, 28: 14–25.
33. Sonka M, Reddy GK, Winniford MD, Collins SM (1997) Adaptive approach to accurate analysis of small diameter vessel in cineangiograms. *IE Trans Med Imaging*, 16: 87–95.
34. Tsutsui H, Schoenhagen P, Crowe TP, Klingensmith JD, Vince DG, Nissen SE, Tuzeu EM (2003) Influence of coronary pulsation on volumetric intravascular ultrasound measurements performed without ECG gating validation in vessel segments with minimal disease. *Int J Cardiovasc Imag*, 19: 51–57.
35. VanBavel E, Spaan JA (1992) Branching patterns in the porcine coronary arterial tree. Estimation of the flow heterogeneity. *Circ Res*, 71: 1200–1212.
36. Wang JZ, Jie B, Welkowitz W, Kostis J, Summlow B (1989) Incremental network analogue model of the coronary artery. *Med Biol Eng Comput*, 27: 416–422.
37. Weber OM, Martin AJ, Higgins CB (2003) Whole-heart steady-state free precession coronary artery magnetic resonance angiography. *Magn Reson Med*, 50: 1223–1228.
38. Zamir M, Phipps S (1988) Network analysis of an arterial tree. *J Bio Mech*, 21: 25–34.
39. Zamir M, Sinclair P (1988) Roots and calibers of the human coronary arteries. *Am J Anat*, 183: 226–234.
40. Zamir M, Phipps S, Langille BL, Wonnacott TH (1984) Branching characteristics of coronary arteries. *Can J Physiol Pharmacol*, 62: 1453–1459.
41. Zamir M (1996) Tree structure and branching characteristics of the right coronary artery in a right dominant human heart. *Can J Cardiol*, 12: 593–599.
42. Zamir M, Chee H (1987) Segment analysis of human coronary arteries. *Can J Cardiol*, 24: 76–84.
43. Zamir M (1988) Distributing and delivering vessels of the human heart. *J Gen Physiol*, 91: 725–735.
44. Zamir M, Chee H (1986) Branching characteristics of human coronary artery. *Can J Physiol Pharmacol*, 4: 21–24.
45. Zole P, Schlesinger MJ, (1938) An injection plus dissection study of coronary artery occlusion and anastomoses. *Am. Heart J*, 15: 528–568.